First Evaluation of Ultrafast (Ground State) Intramolecular Electron Transfer Rate in Solution by NMR Spin−Lattice Relaxation. An Application to Mixed-Valence Biferrocene Monocation (Fe(II), Fe(III))

Akiko Masuda,[†] **Yuichi Masuda,*** **and Yutaka Fukuda**

Department of Chemistry, Faculty of Science, Ochanomizu University, Bunkyo-ku, Tokyo 112, Japan

Received: October 24, 1996; In Final Form: January 2, 1997[⊗]

The rates of the ultrafast intramolecular electron transfer (ET) for mixed-valence biferrocene monocation (Fe(II), Fe(III)) were determined in various solvents and at various temperatures by the ^{1}H NMR spin−lattice relaxation time measurements. The results of the ESR line broadening of biferrocene and ferricenium ions as well as the NMR relaxation measurements indicated that the correlation time responsible for the spin−lattice relaxation time of the cyclopentadienyl protons of biferrocene monocation was approximately equal to the lifetime of electron hopping between the two iron ions, i.e., the inverse of the rate constant of the intramolecular ET. The obtained ET rate constants exceeded 10^{12} s^{-1} at room temperature, e.g., 1.3×10^{12} s^{-1} in acetone at 298 K, and showed significant solvent dependence. The solvent and temperature dependences of the rate constants thus obtained were examined by theories considering the dynamic solvent effect. The obtained rate constants and the temperature dependences were respectively higher and smaller than those predicted by the theories.

1. Introduction

In this decade, remarkable progress in the experimental and theoretical studies of ultrafast chemical processes has provided new aspects for understanding chemical reactions in solution. One of the most important outcomes among these studies is that the importance of contributions of dynamic properties of the solvent to the reaction rates has been proved.[1,2] Particularly for intramolecular electron transfer (ET) reactions, the effect of solvation dynamics is important because of strong coupling between the charge migration accompanied by the ET process and the solvent polarization.[2]

It is necessary that one or more photoexcitation processes (or via photoexcited state(s)) are included in the reaction systems used in studies of ultrafast (intramolecular) ET reactions since the experimental approach has been realized by the recent immediate development of pico- and femtosecond time-resolved pulse laser techniques. These studies have provided us with new information about short-lived intermediates as well as the mechanism of the (dynamic) solvent effect on the rates.[1,2]

Whereas, ultrafast intramolecular ET processes without any photoexcitation (ground state intramolecular ET) are rather general and still fundamental in the fields of chemistry and biology, etc.,[3,4] and are proposed for many inorganic[5] and organic[6] mixed-valence systems. Nevertheless, there has been no quantitative information about the rate constants exceeding 10^{11} s^{-1}; the fastest rates experimentally determined so far were reported for some mixed-valence organic radicals of dinitro and dialdehyde benzene derivatives by ESR line broadening analysis.[7] An analysis of line broadening of vibrational (IR and Raman) spectra or dielectric or microwave relaxation spectra can be theoretically applicable to determine such ultrafast intramolecular ET rates. However, appreciable obstruction of the solvent bands or relaxations usually causes difficulty in analyzing those of the solute (reactant), unless one carries out these experiments in appreciably highly concentrated solutions.[8]

Most of studies on ground state ultrafast ET reactions have been concerned with the ET rates in electron donor−acceptor precursor complexes assumed in the processes of *intermolecular* ET reactions.[9] For example, Weaver et al. systematically studied the ET rates within the precursor complexes of metallocene donor−acceptor couples, $Co(cp)_2{}^0/Co(cp)_2{}^+$ and $Fe(cp)_2{}^0/Fe(cp)_2{}^+$, and presented how the dynamic solvent properties affected the rates.[10] However, in general, some ambiguity exists in quantitative determination of the ET rates within precursor complexes, e.g., experimental difficulty in determining those formation constants. No direct information about geometry or configuration of the precursor complexes causes additional ambiguity in estimating the reaction parameters, such as the reorganization energies and the strength of the electronic coupling between the donor and acceptor.[2c,11]

Thus, a method to quantitatively determine the rates of picosecond order *intramolecular ET* in systems *without any photoexcitation processes* is proposed. In the present study we present such a method by means of NMR spin−lattice relaxation time measurements.

The spin−lattice relaxation time, T_1, depends on the correlation times of fluctuations of magnetic interactions on a nucleus.[12] This fluctuation is caused by various dynamic processes, such as molecular motions (rotational and translational motions)[14] as well as chemical processes.[13] In most cases, chemical processes, however, do not contribute to nuclear spin−lattice relaxations in solution since the relaxations are dominated by faster molecular rotations than the reaction rates.[15] Whereas, for the ultrafast intramolecular ET, the T_1 measurement is expected to be a valuable method for evaluating the ET rate constant exceeding 10^{11} s^{-1} because the fluctuation of the magnetic interaction between a nuclear spin and unpaired electron(s) in an electron donor−acceptor complex by the ET process is fast enough to become an important cause of the NMR spin−lattice relaxation compared with other comparable or slower fluctuations, such as molecular reorientations, whose time scale is usually 10^{-11}−10^{-12} s or longer. (See section 3.1.) Such an application of the spin−lattice relaxation measurements to determine the rates of chemical processes has been limited

---

* To whom correspondence should be addressed.

[†] Present address: Department of Chemistry, Faculty of Science, Tokyo Institute of Technology, Meguro-ku, Tokyo 152, Japan.

[⊗] Abstract published in *Advance ACS Abstracts,* March 1, 1997.

S1089-5639(96)03317-8 CCC: $14.00

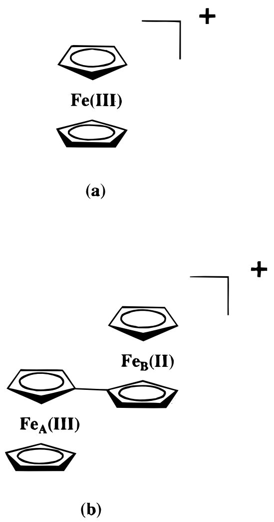

Figure 1. Illustration of ferricenium monocation (a) and mixed-valence biferrocene monocation (b). The formal oxidation states of the two iron atoms in the biferrocene monocation are three for the ferricenium unit ($S = {}^1/_2$) and two for the ferrocene unit ($S = 0$), labeled by Fe_A and Fe_B, respectively. The electron-transfer reaction is represented by $bfc^+(Fe_A(III), Fe_B(II)) \rightleftharpoons bfc^+(Fe_A(II), Fe_B(III))$.

only for some examples;[16,17] most of those are studies on very fast solvent (water)-exchange rates on metal ions with a time scale of 10^{-11} s or shorter.[16]

In the present study, this idea was applied to determine the rate constants of the intramolecular ET of mixed-valence biferrocene (Fe(II), Fe(III)) monocation (see Figure 1) in various solvents and at various temperatures, and the obtained rate constants were examined by several theories considering solvent dynamic properties.

The biferrocene monocation (Fe(II), Fe(III)), bfc^+, is a well-known class II type mixed-valence complex, and the mixed-valence state has been studied by various methods.[18] An ET rate time scale faster than 10^{-7} s was reported for some of the derivatives in their solid state by Mössbauer measurements.[18−20] Although no quantitative information on the ET rate in solution has been reported, a very large rate constant, $k_{et} > 10^{11}$ s^{-1}, of the intramolecular ET reaction is expected by the energy of the IT band maximum (∼5000 cm^{-1}) and the substantially strong electronic coupling between the two mixed-valence states ($Fe_A(II){-}Fe_B(III)$ and $Fe_A(III){-}Fe_B(II)$, see Figure 1), which respectively provide the small barrier (∼15 kJ/mol) and the relatively large transparency coefficient, $\kappa \sim 1$.[10e,18e] Variation in the derivatives of bfc^+ (or bfc) by substitution on the cyclopentadienyl rings[19] or by inserting a bridging group, such as $-CH_2-$ or $-C{=}C-$ between the two ferrocene units,[20] is also important in examining the various theories for the solvent effect on the ET rate because a proper choice of the derivatives allows us to systematically change the reaction parameters, such as the electronic coupling and the outer- and inner-sphere reorganization energies, etc.

2. Experimental Section

Materials. Biferrocene was synthesized by a literature method.[21] The tetrafluoroborate salts of the mixed-valence biferrocene monocation ($bfc^+BF_4^-$) were obtained in the following way.[22] A stoichiometric amount of $AgBF_4$ was added to the solutions of biferrocene dissolved in a minimum amount of dry nitromethane. After removing the resultant silver, nitromethane was evaporated under vacuum. The obtained salts of biferrocene monocation were dried under vacuum. The hexafluorophosphonium salt of ferricenium ion ($fc^+PF_6^-$) was obtained by adding aqueous NH_4PF_6 to the solution of ferrocene (Aldrich Co. Ltd.) dissolved in sulfuric acid after oxidation. All the above procedures were carried out under dry argon atmosphere.

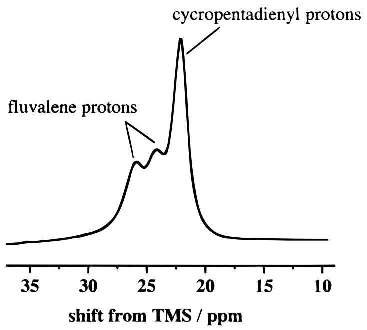

Figure 2. ^1H NMR spectra of $bfc^+BF_4^-$ in acetone at 20 °C.

Spectroscopic Measurements. The ^1H NMR were obtained on a JEOL GX-270 Fourier-transform spectrometer operating at 270 MHz. The spin−lattice relaxation time, T_1, and the spin−spin relaxation time, T_2, were determined by the inversion-recovery method and the CPMG method, respectively. The chemical shifts were determined by use of TMS as internal reference. The measurements were performed using 5 mm (o.d.) cylindrical tubes, and the temperature was controlled within ±0.5 °C. The X-band ESR spectra were measured on a JEOL FE-ESR spectrometer at 9.1 GHz microwave frequency. The UV, visible, and near-IR spectra were measured with a HITACHI 340 spectrophotometer.

The sample solutions were degassed under vacuum by two freeze−pump−thaw cycles and were torch-sealed before measurements. The deuterated solvents (>99.9 atom % provided by Isotec Inc.) were used for the NMR measurements without further purification. The protiated solvents for the other measurements were dried and distilled by the usual methods before use.

The measurements of NMR and ESR for the ferricenium and the biferrocene monocation salts solutions were carried out at concentrations of 1−2 mM of the salts, unless otherwise noted. In several solvents, the concentration dependences of the NMR T_1, T_2, and shifts were measured below a few millimolar concentrations of the salts. No significant concentration dependence was observed. Thus, we assumed no effect of interaction of the counterion (BF_4^- or PF_6^-) on the observed relaxation times and shifts below a few millimolar concentrations of the salts.

In the proton NMR spectra of bfc^+ three sets of proton signals (two fulvalene and one cyclopentadienyl proton signals with 2:2:5 intensity) were partially overlapped as shown in Figure 2. Each peak intensity and position to obtain the proton relaxation times (T_1 and T_2) and the shift were determined by a deconvolution method assuming its Lorentzian line shape.

3. Results and Discussion

3.1. Basic Idea To Evaluate the Ultrafast Intramolecular ET Rate Constants. In this section, we describe the basic idea of our first attempt to determine the ultrafast (ground state) intramolecular ET rate.

Generally, a nuclear spin−lattice relaxation is caused by fluctuations of magnetic interactions on the nucleus. In the case of the longitudinal relaxation of a nuclear spin, *I*, in an electron donor−acceptor complex, the interaction between the nuclear spin, *I*, and the electron spin, *S*, in the complex significantly contributes to the nuclear relaxation (e.g., in the bfc^+ system, the interaction between an electron spin ($S = {}^1/_2$) on Fe(III) and a certain proton ($I = {}^1/_2$) of the cyclopentadienyl ring in the fc$^+$ unit dominates the magnetic relaxation of the nuclear spin, *I;* see section 3.2). This relaxation time, $T_{1\mathrm{para}}$, mainly consists of two terms: one is caused by the magnetic dipolar interaction and the other by the hyperfine interaction with the electron spin and are denoted by $T_{1\mathrm{dip}}$ and $T_{1\mathrm{hyp}}$, respectively. $T_{1\mathrm{para}}$ is then represented by[23,24]

$$T_{1\mathrm{para}}{}^{-1} = T_{1\mathrm{dip}}{}^{-1} + T_{1\mathrm{hyp}}{}^{-1} \qquad (1)$$

and

$$T_{1\mathrm{dip}}{}^{-1} = K_{\mathrm{dip}}[3\tau_{\mathrm{c1}} + 7\tau_{\mathrm{c2}}/(1 + \omega_{\mathrm{S}}{}^2\tau_{\mathrm{c2}}{}^2)] \qquad (2a)$$

$$T_{1\mathrm{hyp}}{}^{-1} = K_{\mathrm{hyp}}[\tau'_{\mathrm{c2}}/(1 + \omega_{\mathrm{S}}{}^2\tau'_{\mathrm{c2}}{}^2)] \qquad (2b)$$

$$K_{\mathrm{dip}} = (2/15)(S(S+1))\,\gamma_{\mathrm{H}}{}^2 g^2\beta^2 r_{\mathrm{IS}}{}^{-6} \qquad (3a)$$

$$K_{\mathrm{hyp}} = (2/3)(S(S+1))(A/\hbar)^2 \qquad (3b)$$

where ω_{S} is the Larmor frequencies of the electron spin; g^2 is given by the parallel and perpendicular g values of the electron spin, $g_{\|}$ and $g_{\perp}$, respectively, with the relation, $g^2 = (g_{\|}{}^2 + 2g_{\perp}{}^2) + g_{\|}{}^2\cos^2\theta + g_{\perp}{}^2\sin^2\theta$, where θ indicates the angle between the main axis of the **g** tensor and the vector connecting the observed nuclear spin and the electron spin. γ_{H}, β, A, and r_{IS} respectively represent the gyromagnetic ratio of the observing nucleus, the Bohr magneton, the hyperfine coupling constant, and the distance between the nucleus and the electron spin. τ_{c}, i.e., τ_{c1} and τ_{c2} in eq 2a and τ'_{c2} in eq 2b are the correlation times of the fluctuations of the magnetic interactions for the respective magnetic relaxations (see below). These fluctuations are usually caused by the molecular reorientational motion and the electron spin relaxation.[12,23] Whereas, if a rapid ET process exists in a system, the electron hopping from one side to another side also causes an additional fluctuation of the magnetic interaction between the electron spin and the nucleus observing the NMR, e.g., for the relaxation of a proton of the cyclopentadienyl ring in the fc$^+$ unit of bfc$^+$ by the dipolar interaction, the local magnetic field at the proton caused by the electron spin on the Fe(III) ion in the fc$^+$ unit is changed (almost diminished) by the electron transfer from the other iron atom to the iron atom (from Fe$_{\mathrm{B}}$ to Fe$_{\mathrm{A}}$ in Figure 1), because the interaction, i.e., the inverse of the relaxation time, $T_{1\mathrm{dip}}{}^{-1}$, is proportional to $r_{\mathrm{IS}}{}^{-6}$ as shown in eq 2a. Then the correlation times in eqs 2a and 2b are expressed by[23]

$$\tau_{\mathrm{c1}}{}^{-1} = \tau_{\mathrm{r}}{}^{-1} + T_{1\mathrm{e}}{}^{-1} + k_{\mathrm{et}} \qquad (4a)$$

$$\tau_{\mathrm{c2}}{}^{-1} = \tau_{\mathrm{r}}{}^{-1} + T_{2\mathrm{e}}{}^{-1} + k_{\mathrm{et}} \qquad (4b)$$

$$\tau'_{\mathrm{c2}}{}^{-1} = T_{2\mathrm{e}}{}^{-1} + k_{\mathrm{et}} \qquad (4c)$$

where τ_{r}, $T_{1\mathrm{e}}$, $T_{2\mathrm{e}}$, and k_{et} denote the reorientational correlation time, the spin−lattice and the spin−spin relaxation time of the electron spin, and the ET rate constant, respectively. If the ET rate is comparable or faster than the molecular reorientation and the electron spin relaxation, k_{et} significantly contributes to $\tau_{\mathrm{c}}{}^{-1}$. The rotational correlation time, τ_{r}, is usually 10^{-12}−10^{-11} s or longer even for small molecules.[14] A similar situation in $T_{1\mathrm{e}}$ or $T_{2\mathrm{e}}$, i.e., $T_{1\mathrm{e}}$, $T_{2\mathrm{e}} > 10^{-12}$−$10^{-11}$ s, is observed for a considerable part of the first-row transition-metal complexes and most organic radicals.[23,24] Thus, intramolecular ET rate constants, k_{et}, exceeding 10^{11}−10^{12} s^{-1} can be evaluated if the τ_{c} value is determined from a measured T_1 under the condition where the $\tau_{\mathrm{r}}{}^{-1}$ and $T_{2\mathrm{e}}{}^{-1}$ (or $T_{1\mathrm{e}}{}^{-1}$) values are not much larger than the k_{et} value.

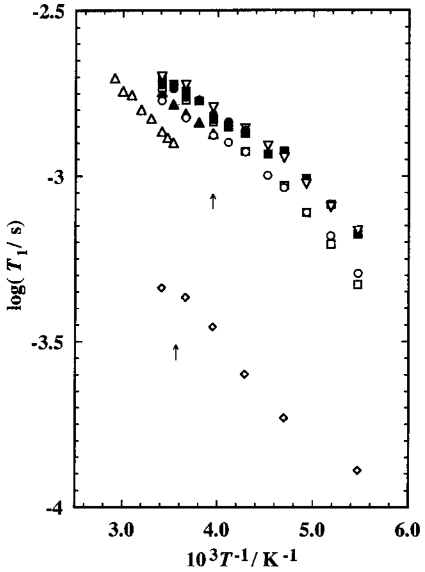

Figure 3. Temperature dependences of the observed T_1 of cyclopentadienyl protons of the biferrocene monocation in various solvents: ○, acetone; ●, acetonitrile; ▽, dichloromethane; ▲, nitromethane; △, nitrobenzene; ■, methanol; □, ethanol; ◇, ferricenium ion in acetone.

3.2. Evaluation of the Intramolecular ET Rate Constant of bfc$^+$. In this section, the concept described in the previous section is applied to evaluate the intramolecular ET rate constant, k_{et}, of the mixed-valence biferrocene monocation (bfc$^+$). The procedure is divided into two steps. The first is an evaluation of the correlation times, τ_{c}, in eq 2 from the observed longitudinal relaxation times of the cyclopentadienyl proton of bfc$^+$. In the second step, the k_{et} values are determined from the obtained correlation times, τ_{c}, according to eq 4, by estimating τ_{r} and $T_{1\mathrm{e}}$ (or $T_{2\mathrm{e}}$).

Evaluation of τ_{c}. T_1 values of the cyclopentadienyl protons of bfc$^+$ and bfc were measured in various solvents and at various temperatures. Similar measurements were also carried out for fc$^+$ and fc in order to estimate the electron spin relaxation times, $T_{1\mathrm{e}}$ or $T_{2\mathrm{e}}$ (see below). Because the observed $T_1{}^{-1}$ values for bfc$^+$ and fc$^+$ were much larger than those for bfc or fc, respectively, as shown in Table 1, the contribution of the interaction with the unpaired electron (the paramagnetic term) dominates the cyclopentadienyl proton relaxations.[25] The observed temperature dependences of the T_1 values of bfc$^+$ in various solvents are shown in Figure 3.

In order to evaluate the correlation times represented in eqs 2a and 2b from the observed T_1 values, the K_{dip} and K_{hyp} values in the dipolar and hyperfine relaxation terms, respectively, in eqs 3a and 3b were determined as follows.

The g values, i.e., $g_{\|}$ and $g_{\perp}$, in K_{dip} for bfc$^+$ were determined by the ESR measurements for the frozen acetone solutions of ca. 1 mM bfc$^+$(BF$_4^-$) in the temperature range 78−170 K. Similar measurements were carried out in different solvents. The obtained values are listed in Table 1 together with those for fc$^+$ from the literature.[18,26] There was only slight difference between the values in different solvents and at temperatures. Consequently, we use the $g_{\|}$ and $g_{\perp}$ values in acetone for those in different solvents used in the NMR measurements. r_{IS} was assumed to be a distance between a cyclopentadienyl proton and the Fe atom in the ferricenium unit of bfc$^+$ and was taken to be 2.85 Å based on the X-ray crystal data of the bfc$^+$I$_3^-$ salt, assuming 1.09 Å for the C−H bond length.[18d,e] The $g_{\|}$

TABLE 1: NMR and ESR Parameters for Ferrocene and Biferrocene and Their Monocations[a]

	$g_{\parallel}$	$g_{\perp}$	$(\Delta\nu/\nu_o)_{obs}$,[h] ppm	$(\Delta\nu/\nu_o)_{para}$,[j] ppm	$(\Delta\nu/\nu_o)_{dip}$,[k] ppm	$(\Delta\nu/\nu_o)_{hyp}$,[l] ppm	$A/\hbar$,[m] 10^6 s^{-1}
ferrocene			4.16				
ferrocene$^+$PF$_6^-$	4.35	1.26[b]	36.8	32.6	1.76	30.84	5.80
	4.55	1.15[c]					
biferrocene			3.99				
			4.17[i]				
			4.35[i]				
biferrocene$^+$BF$_4^-$	3.40	1.63[d]	22.1	36.3	1.75	34.75	5.76
	3.38	1.67[e]					
	3.35	1.60[f]					
	3.20	1.52[g]					

	T_{1obs}, s	T_{1para},[n] s	T_{1dip},[o] s	T_{1hyp},[p] s	τ_c,[q] s	$\tau_{r(eff)}$,[r] s	τ_r,[s] s
ferrocene	29.0					4.2×10^{-11}	
ferrocene$^+$PF$_6^-$	4.6×10^{-4}	4.6×10^{-4}	4.7×10^{-4}	2.2×10^{-2}	7×10^{-12}		4.2×10^{-11}
biferrocene	19.9					6.3×10^{-11}	
	11.7[i]					10.1×10^{-11} [i]	
	13.5[i]					9.5×10^{-11} [i]	
biferrocene$^+$BF$_4^-$	17.1×10^{-4}	8.5×10^{-4}	8.7×10^{-4}	3.7×10^{-2}	0.89×0^{-12}		7.0×10^{-11}

[a] Values for the cycropentadienyl protons in acetone or acetone-d_6 at 293 K unless otherwise noted. [b] Measured in the frozen acetone solution at 20 K (ref 25). [c] Measured for the powder sample at 4 K (ref 18). [d] Measured in the frozen acetone solution at 98 K. [e] Measured in the frozen acetone solution at 170 K. [f] Measured in the frozen methanol solution at 170 K. [g] Measured for the powder sample at 98 K. [h] Shifts from TMS as internal reference. [i] Values for the fulvalene protons. [j] See ref 52. [k] Values calculated by eq A1b with the g values (in Table), r_{IS} (=2.85 Å), and θ (=53.9°), whose values are taken from ref 18d,e. [l] Values calculated from $\Delta\nu/\nu_o - (\Delta\nu/\nu_o)_{dip}$. [m] Values calculated from $(\Delta\nu/\nu_o)_{hyp}$ with eq A1c. Details in text. [n] Values for fc$^+$ and bfc$^+$ are assumed to be respectively equal to T_{1obs} and $T_{1obs}/2$ of the cp protons in fc$^+$ and bfc$^+$. (See ref 25.) [o] Values calculated according to eqs 1 and 3a assuming a same τ_c value for T_{1dip} and T_{1hyp}. (See ref 27.) [p] Values calculated according to eqs 1 and 2b assuming a same τ_c value for T_{1dip} and T_{1hyp}. (See ref 27.) [q] Details in text. [r] Values calculated for observed T_1 of the cp ring protons according to eq 5. [s] Reorientational correlation times responsible for T_{1dip}, which are rotations of a vector connecting a cyclopentadienyl proton and the Fe(III) ion in the fc$^+$ unit of bfc$^+$. τ_r of bfc$^+$ is assumed to be equal to that for bfc.

TABLE 2: NMR Shift of Cyclopentadienyl Protons of bfc$^+$BF$_4^-$ at 293 K

solvent[a]	$(\Delta\nu/\nu_o)_{para}$/ppm[b]	$A/\hbar$/s^{-1} [c]	solvent[a]	$(\Delta\nu/\nu_o)_{para}$/ppm[b]	$A/\hbar$/s^{-1} [c]
acetone	36.3	5.76	nitrobenzene	35.0	5.55
acetonitrile	35.2	5.58	methanol	35.4	5.62
dichloromethane	37.2	5.90	ethanol	35.9	5.70
nitromethane	36.0	5.71			

[a] Deuterated solvents were used. [b] Twice values of the difference between $(\Delta\nu/\nu_o)_{obs}$ for bfc$^+$ and for bfc. See ref 26. [c] Values calculated with eq A1c assuming $(\Delta\nu/\nu_o)_{para} = (\Delta\nu/\nu_o)_{hyp}$.

and $g_{\perp}$ values and the r_{IS} value thus obtained gave 1.29×10^{15} s^{-2} as the K_{dip} value.

The hyperfine coupling constant between the cyclopentadienyl protons of fc$^+$ unit and the electron spin on the Fe(III) ion in bfc$^+$ (A in eq 3b) was estimated from the ^{1}H NMR shift. Details of the procedure to determine the A value are given in the Appendix. The obtained $A/\hbar$ value was 1.83×10^6 s^{-1} for bfc$^+$ in acetone at 293 K. Similar procedures were carried out in the other solvent. There was no significant difference in the obtained A values. The NMR shift and the A values obtained in the solvents other than acetone are listed in Table 2. The K_{hyp} value calculated with the A value was 3.04×10^{13} s^{-2} and was much smaller than the K_{dip}. This indicates that the $T_{1hyp}{}^{-1}$ term is negligibly small to the $T_{1para}{}^{-1}$ term, that is, $2T_{1obs}{}^{-1} = T_{1para}{}^{-1} \approx T_{1dip}{}^{-1}$ [25,27] (see Table 1).

For estimation of the correlation time, τ_{c1} or τ_{c2}, from $T_{1dip}{}^{-1}$ ($=T_{1para}{}^{-1}$), we made some simplifications for eq 2a: (i) when $T_{1e} = T_{2e}$ or $k_{et} + \tau_r{}^{-1} \gg T_{2e}{}^{-1}$ ($> T_{1e}{}^{-1}$), τ_{c2} is equal to τ_{c1}, (ii) when $k_{et} + \tau_r{}^{-1} \ll T_{2e}{}^{-1}$ and $T_{1e} \gg T_{2e}$, i.e., $\tau_{c1} \gg \tau_{c2}$, $T_{1dip}{}^{-1}$ is approximated by $3K_{dip}\tau_{c1}$. In the both cases the inside of the brackets in eq 2a approximately depends only on τ_{c1}. Thus, the correlation times, τ_{c1}, are estimated to be 10^{-12} s^{-1} or less at room temperature in most of the solvents with the K_{dip} value above obtained, e.g., 0.9×10^{-12} s for $\tau_{c1} = \tau_{c2}$ and 1.3×10^{-12} s for $\tau_{c1} \gg \tau_{c2}$ in acetone at 293 K.[28]

A loose shoulder was observed in the temperature dependence of T_1 in each solvent in the temperature range 240 − 290 K (labeled by an arrow in Figure 3). These shoulders are probably brought by the condition $\omega_S\tau_c = 1$, as shown by eq 2a; therefore, the τ_c values in the temperature range should be around 1.1×10^{-12} s, which is the inverse of the resonance frequency of the electron spin under the magnetic field (6.8 T) for the NMR measurements. The τ_c values obtained above satisfied this condition, indicating that values of the parameters A, $g_{\parallel}$, $g_{\perp}$, etc., used in the present study are appropriate.[29]

Determination of k_{et} from τ_c. The correlation time, τ_{c1}, obtained above consists of the reorientational correlation time, τ_r, and the electron spin relaxation time, T_{1e}, as well as k_{et} as shown in eq 4a.

The rotational correlation time responsible for T_{1dip} of the cyclopentadienyl protons in the fc$^+$ unit of bfc$^+$ corresponds to that of the vectors connecting between the electron spin, i.e., the Fe(III) ion in bfc$^+$ and the protons.[12,23] The correlation time was estimated from the ^{1}H T_1 measurements for bfc assuming that the τ_r value of bfc$^+$ was similar to that of bfc.[30] This assumption is retained by studies on the rotational motion of various complex ions in the solutions. These studies presented the negligible effect of the ionic charge of the complex ions on the rotational correlation times when the ionic radii of the complex ions are similar to that of bfc (r(bfc) = ∼8 Å).[14b,31] The observed T_1 values of the cyclopentadienyl and the fulvalene protons in bfc are related to the rotational correlation times by the following equation[12]

$$(1/T_1)_{obs} = (3/4)n\gamma_H{}^4\hbar^2 r_{HH}{}^{-6}\tau_{r(eff)} \qquad (5)$$

where r_{HH} and n denote the distance between the observing and the adjacent protons and the number of the adjacent protons,

TABLE 3: Spin−Lattice Relaxation Times and Reorientational Correlation Times of Biferrocene

		$T_{1\mathrm{obs}}$/s			
solvent[a]	temp/K	cyclopentadienyl protons	fulvalene protons		$\tau_r/10^{-11}$ s[b]
acetone	299	22.0	13.2	14.5	6.3
	293	19.9	11.7	13.5	7.0
	240	11.0	5.6	6.6	14
	210	7.0	3.2	3.9	24
acetonitrile	305	20.1	12.1	13.5	6.8
	293	17.6	10.5	10.9	7.8
	250	7.2	4.2	4.9	18
dichloromethane	293	18.0	10.9	11.5	7.6
	260	14.0	8.2	8.9	10
	210	7.5	4.4	5.0	17
nitromethane	293	14.0	8.1	8.7	11
	260	11.0	5.2	5.9	15
nitrobenzene	320	7.0	3.4	3.8	24
	293	4.0	1.8	2.0	44
	270	2.8	1.2	1.4	66
methanol	293	11.0	5.6	6.2	14
	230	4.0	1.9	2.1	42
	210	2.8	1.3	1.5	63
ethanol	310	10.0	5.5	5.9	15
	293	4.0	1.9	2.1	42
	240	2.3	1.1	1.2	70

[a] Deuterated solvents were used. [b] See ref 30.

respectively. $\tau_{r(\mathrm{eff})}$ indicates the rotational correlation times of a vector connecting the protons. The obtained $\tau_{r(\mathrm{eff})}$ values in eq 4 for the cyclopentadienyl and fulvalene protons are listed in Tables 1 and 3. The rotational correlation time for $T_{1\mathrm{dip}}{}^{-1}$ of the cyclopentadienyl protons in the fc$^+$ unit of bfc$^+$, which corresponds to that for the rotation of a vector connecting the proton and the Fe(III) ion, was determined from the $\tau_{r(\mathrm{eff})}$ values obtained above[30] and is also listed in Tables 1 and 3. The obtained τ_r in acetone at 293 K is much longer than that of the τ_{c1} value estimated above, i.e., the rotational motion does not contribute to τ_{c1}.

Fast electron spin relaxation in bfc$^+$ in solution makes it difficult to obtain the ESR signal although the ESR spectra give information on the electron spin relaxation time, T_{1e} or T_{2e}. Therefore, T_{1e} of bfc$^+$ was estimated on the basis of that of fc$^+$, which was determined with the measured ^{1}H T_1 value of fc$^+$ as follows.

The $T_{1\mathrm{para}}$ of fc$^+$ is approximately equal to $T_{1\mathrm{dip}}$, which depends only on τ_{c1} as in bfc$^+$. (See Table 1.) Then, the T_{1e} value of fc$^+$ can be determined from the τ_{c1} and the τ_r value for fc$^+$, which are obtained in a similar manner as bfc$^+$, because the correlation times of fc$^+$ are represented by $\tau_r{}^{-1}$ and $T_{1e}{}^{-1}$, i.e., by eq 4 without the k_{et} term. Thus, τ_{c1} for fc$^+$ is estimated to be, e.g., ca. 7×10^{-12} s in acetone at 293 K. Since the correlation time is much smaller than τ_r ($\approx 4 \times 10^{-11}$ s) for fc$^+$, τ_{c1} is equal to T_{1e}. Then, the T_{1e} value for bfc$^+$ relative to that for fc$^+$ is estimated as follows.

The ESR line widths for bfc$^+$ in both the frozen acetone and methanol solution were ca. 500 G at 170 K and ca. 300 G at 78 K at 9.1 GHz microwave frequency. On the other hand, the ESR for fc$^+$ is reported only at 20 K with ~500 G line width at 9.2 GHz (in the frozen acetone solution and for the powdered sample), and it is difficult to observe the ESR signals at higher temperature because of the short electron spin relaxation time.[18b,26] Cowan et al.[18b] analyzed the $g_\parallel$ and $g_\perp$ values and the magnetic susceptibility data for fc$^+$ and bfc$^+$ according to a model by Maki et al.[32] and concluded that this longer relaxation time of bfc$^+$ than fc$^+$ was attributed to the larger energy splitting between the two Kramer's doublets of the orbitally degenerate configuration, $^2E_{2g}[(a_{1g})^2(e_{2g})^3]$, caused by larger distortion from the D_5 symmetry in the fc$^+$ unit in bfc$^+$. In this case, the electron spin relaxation time, T_{1e}, is proportional to $(\delta/\xi)^2$, where δ and ξ denote the energy splitting and the spin−orbit coupling constant, respectively.[33] More than 3 times larger δ/ξ for bfc$^+$ than fc$^+$ [18b, 26] results in more than 10 times longer relaxation times of bfc$^+$ if the correlation times responsible for the relaxations are similar between bfc$^+$ and fc$^+$. Thus, T_{1e} of bfc$^+$ is estimated to be more than $\sim 7 \times 10^{-11}$ s.

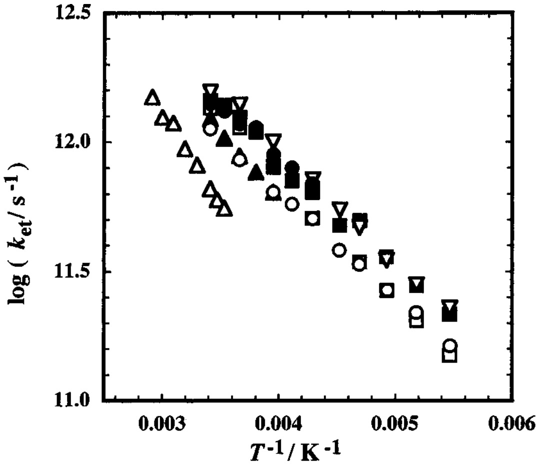

Figure 4. Temperature dependences of the observed k_{et} in various solvents: ○, acetone; ●, acetonitrile; ▽, dichloromethane; ▲, nitromethane; △, nitrobenzene; ■, methanol; □, ethanol.

Consequently, the T_{1e} and τ_r values of bfc$^+$ are much longer than τ_{c1} of bfc$^+$, i.e., $\tau_{c1}{}^{-1} \sim k_{et}$. Similar procedures were applied in different solvents and at different temperatures,[34] and the same results were obtained. Thus, the k_{et} values can be directly determined from the observed T_1 of the cyclopentadienyl protons in bfc$^+$ using the condition $\tau_{c1}{}^{-1} = k_{et}$.

The ET rate constants of bfc$^+$, k_e, in various solvents and at various temperatures were calculated with the observed T_1 values using the relation $\tau_{c1}{}^{-1} = k_{et}$. The obtained k_{et} values at room temperature exceeded 10^{12} s^{-1} in most solvents. These rate constants are the first example of the *thermal-induced (ground state) intramolecular ET reaction exceeding 10^{12} s^{-1}*.

The present method of determining ET rates requires only the condition that the time scale of the reorientational motion and the electron spin relaxation do not appreciably exceed k_{et}. Therefore, the method should extensively contribute to studies for picosecond order ET processes, since ultrafast intramolecular ET in the ground state is quite common for class II mixed-valence systems.

3.2. Dynamical Solvent Effect on k_{et}. *Estimation of Reaction Parameters.* The obtained k_{et} values were 10^{12} s^{-1} or more at room temperature and showed substantial solvent dependence as shown in Figure 4. Hereafter, the solvent effect, particularly its dynamic effect on thus-obtained k_{et} values, is examined. The solvent dynamic effect is often discussed with the preexponential factor, ν_n, in the following transition state theory (TST)-like formula,[2]

$$k_{et} = \nu_n \exp(-\Delta G^*/k_B T) \tag{6}$$

where ΔG^* and ν_n represent the free energy of the barrier and the preexponential factor, respectively. ΔG^* consists of the inner- and outer-sphere (solvent) reorganization energies denoted by λ_{is} and λ_{os}, respectively, and the electronic coupling between the mixed-valence states (Fe$_A$(II)Fe$_B$(III) and Fe$_A$(III)Fe$_B$(II)), H_{12}, with the relation[2]

$$\Delta G^* = \lambda/4 - H_{12}, \quad \lambda = \lambda_{is} + \lambda_{os} \tag{7}$$

TABLE 4: Observed Rate Constants and Reaction Parameters for Intramolecular ET Reaction of bfc$^+$ in Various Solvents (298 K)

solvent	λ_{os}, kJ/mol	λ_{is},[a] kJ/mol	ΔG^*,[b] kJ/mol	k_{et}, 10^{12} s^{-1}	ν_n, 10^{13} s^{-1}
acetone	60.6	7.13	10.9	1.25	3.02
acetonitrile	60.9	7.13	11.0	1.58	3.94
dichloromethane	52.9	7.13	9.0	1.77	1.58
methanol	56.9	7.13	10.0	1.74	2.44
ethanol	59.9	7.13	10.7	1.53	1.89
nitromethane	58.4	7.13	10.4	1.45	3.07
nitrobenzene	55.7	7.13	9.7	0.84	1.44

[a] The values calculated from the Raman (ref 36) and the X-ray crystal data (ref 18d,e) in common with all the solvents. [b] The values calculated according to eq 7 assuming H_{12} = 6.0 kJ/mol in common with all the solvents (see text).

In order to evaluate the ν_n values in eq 6, the parameters, λ_{os}, λ_{is}, and H_{12}, i.e., ΔG^*, were estimated as follows.

The λ values in the various solvents used in the present experiments were determined by the IT band maximum frequency.[10a,35] The λ_{is} value is calculated from the cyclopentadienyl−Fe distance and the stretching force constants of the fc and fc$^+$ unit in bfc$^+$ by the X-ray crystal structure and the Raman scattering data,[18b,36] respectively, assuming no solvent dependence. The H_{12} value was determined from the IT band intensity.[10e]

The obtained reaction parameters are listed in Table 4.[37] The much larger λ_{os} values compared with λ_{is} indicate that the solvent reorganization dominates the barrier of the present ET reaction.

Dynamical Solvent Effect on k_{et}. The importance of the solvent dynamic effect on the ET rate has been particularly demonstrated for the ET reaction with a low reaction barrier, i.e., the ultrafast reaction by recent pico- and femtosecond pulse laser experiments.[1,2] Such a dynamic solvent effect is also expected for the present system because of the low barrier height ($\Delta G^* = (4-5)RT$ at room temperature) and the picosecond time scale ET rate as shown in Table 4. The solvent dynamic effect is often discussed in the solvent dependence of the preexponential factor, ν_n, in eq 6.[2] A clear solvent dependence of the ν_n values obtained in various solvents at 298 K as shown in Table 4 indicates the existence of the solvent dynamical effect on the rates.

In order to examine the solvent dynamical effect, the observed k_{et} or ν_n values were compared with those calculated according to the following two models.

(a) For the present system, the electronic coupling, H_{12}, is considerably large ($H_{12} \sim 3k_BT$ at room temperature). Then, the roundness of the barrier top is sufficient to be affected by dielectric solvent friction when the reaction trajectory passes through the barrier so that this process becomes rate determining.[2] In such a case, the preexponential factor, ν_n, can be approximated as the inverse of longitudinal dielectric relaxation time, τ_L^{-1}, regarding the solvent as Debye continuum.[2,38]

(b) An effect of the internal vibration on the ET rate as well as the solvent dielectric friction is considered by Sumi−Marcus−Nelder in their two-dimensional model (SMN model),[39] and the validity of the model has been proved in various reaction systems in solutions.[2,9,40,41] In this model, the reaction is separated into two processes: (i) the system diffuses suffering solvent dielectric friction along the solvent polarization axis, z_s, and (ii) at a certain position on the solvent coordinate the system reacts along the internal vibrational coordinate, z_i, with the TST rate with a given barrier height. Numerical calculations of k_{et} of the present system were carried out based on an analytical formula for the rate constant for a reversible reaction given by Zhu et al.[42]

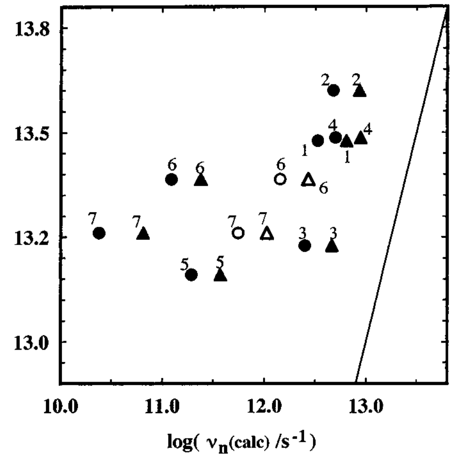

Figure 5. Plots of observed preexponential factors, ν_n, against those calculated at 298 K. Closed circles and triangles indicate the plots for the calculated values assuming $\nu_n = \tau_L^{-1}$ and based on Sumi−Marcus−Nelder model, respectively. Open symbols indicate the values for the fast relaxation component of the dielectric relaxations of alcohols, which are assigned to the OH group reorientation (see text). The solid line represents the slope of unity. 1, acetone; 2, acetonitrile; 3, dichloromethane; 4, nitromethane; 5, nitrobenzene; 6, methanol; 7, ethanol.

The calculated ν_n values and the temperature dependences of k_{et} were plotted against those observed in Figures 5 and 6, respectively.

A plot for the values in acetone, acetonitrile, dichloromethane, and nitromethane, assuming $\nu_n = \tau_L^{-1}$ (model a), showed a slight correlation as shown by closed circles in Figure 5.[43] (Quite different behavior of the plot in alcohols is discussed later.) The experimentally obtained ν_n values were, however, nearly 1 order of magnitude larger than those of τ_L^{-1}, and the observed temperature dependences of k_{et} were smaller than those calculated as shown in Figure 6a. Similar results were also obtained in the comparison between the observed and the calculated ν_n values by the SMN model as shown by closed triangles in Figure 5.

Thus, the dielectric friction regarding solvent as dielectric continuum only partially contributes to the rate-determining process. More than 1 order of magnitude higher ν_n values than τ_L^{-1} and the small temperature dependences in k_{et} also cannot be explained by considering an effect of the internal vibration treated by the SMN model, where the calculated ν_n values are only 2−3 times larger than those assuming $\nu_n = \tau_L^{-1}$ in all the solvents since the system is close to a narrow window limit, i.e., the small contribution of λ_{is} to λ (ca. 0.2) in the present system.[41]

Such ET rates exceeding solvation time ($\sim\tau_L$) and the weak temperature dependences are recently reported for photoinduced (back) electron-transfer reactions with large driving forces,[44,45] and the solvent and temperature dependences of the rates are successfully explained by considering the highly vibrationally exited states, as escape routes of the reactions, which are quantum mechanically treated according to a theory proposed by Jortner−Bixson.[46] However, for symmetric ET reactions such as the present bfc$^+$ system, this effect is quite minor because the utilization of the vibrational excited state as a pathway for the reaction is effective only when an ET system is in a Marcus inverted region as in the above back ET systems.[44−46]

The obtained ν_n values in alcohols were more than 2 orders of magnitude larger than those calculated as shown in Figure 5. Such appreciable larger rates experimentally observed in alcohols than those expected from the Debye dielectric longitudinal relaxation times are also reported for other chemical

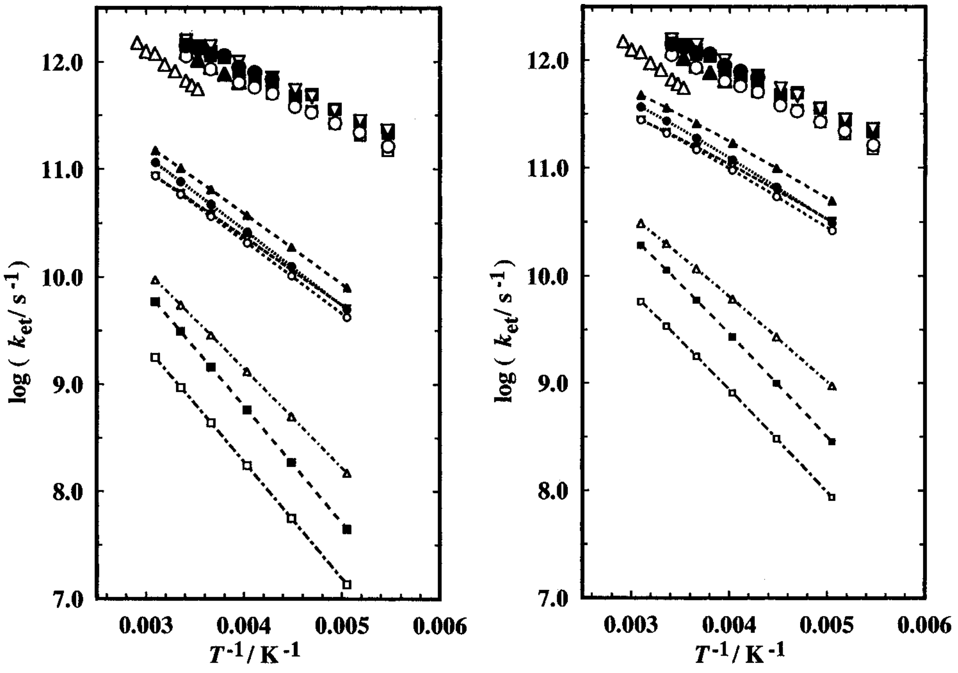

(a) (b)

Figure 6. A comparison of the temperature dependences of observed k_{et} (large symbols) with the calculated values (small symbols) in various solvents. (a) Plot for values assuming $\nu_n = \tau_L^{-1}$ and (b) based on Sumi−Marcus−Nelder model (see text): ○, acetone; ●, acetonitrile; ▽, dichloromethane; ▲, nitromethane; △, nitrobenzene; ■, methanol; □, ethanol.

processes and time-dependent fluorescence Stokes shifts and are attributed to the non-Debye multiple relaxation behavior of alcohols,[47] i.e., one or two minor relaxation components around 1 order of magnitude shorter than the major component are observed in recent microwave experiments and are assigned to local motions such as the OH group reorientation.[48] The plots for the alcohols considering such components with shorter relaxation times (open symbols in Figure 5) approach the trend of the other solvents, indicating that the rapid and local solvent dynamics probably contributes to the friction for the barrier crossing rather than the slower main relaxation component.

For the other solvents, such shorter time scale fluctuations other than the main component relaxation as solvent continuum conceivably contribute to the barrier crossing dynamics in bfc$^+$ with the large ET rates or the preexponential factors of bfc$^+$. For example, ultrafast solvent relaxations below 10^{-12} s have been reported by recent subfemtosecond time-dependent dynamic fluorescence Stokes shift and Kerr relaxation experiments;[1b,48b,c,49,50] in the case of acetonitrile, ∼0.1 ps relaxation(s) comprise a considerable component of the total solvent polarization.[49a,b,50] If such a fast solvent fluctuation is responsible for the barrier-crossing dynamics of the electron transfer in bfc$^+$, the expected ET rate or preexponential factor increases and approaches those experimentally obtained. Such fast solvent relaxations by inertial and local solvent dynamics may be important in controlling the ET rates of the present bfc$^+$ system although it is difficult numerically to estimate the effect because of limitation of the available data and their considerable probe dependences.[48b,49,50]

4. Conclusion

The intramolecular ET rate constants of bfc$^+$ were determined in various solvents at various temperatures by measurements of the NMR spin−lattice relaxation times of the cyclopentadienyl protons. The dipolar term was dominant for the spin−lattice relaxation, and the inverse of the correlation time was approximately equal to the ET rate constant, k_{et}. Thus, obtained k_{et} values exceeded 10^{12} s^{-1} at 298 K in most of solvents.

The preexponential factors, which were determined with the observed rate constants and the reaction parameters estimated by the IT band spectra and the metal−ligand stretching Raman bands, indicated significant solvent dependence. The calculated ET rate constants or the preexponential factors considering solvent dielectric friction for the barrier crossing assuming the solvents as Debye continuum gave much smaller values than those observed. The theory also overestimated the temperature dependences. An application of Sumi−Marcus−Nelder model showed somewhat better prediction for the rate constants and their temperature dependences. The obtained preexponential factors or the rate constants 5 times or more larger than those predicted by the theories suggested contribution of fast component(s) of solvent relaxation by the local or inertial dynamics.

Acknowledgment. We thank Prof. S. Nakashima (Hiroshima University) for providing the biferrocene sample. This work was partially supported by a Grant-in-Aid for Scientific Researches, No. 06640717 and No. 08454235, for the Ministry of Education, Science and Culture.

5. Appendix

The procedure for evaluating the hyperfine coupling constant, *A*, is given in this section. Assuming axial symmetry for the **g** tensor and the isotropic hyperfine interaction, the shift caused by the interaction with the electron spin, $(\Delta\nu/\nu_0)_{para}$, is represented by[23,51]

$$(\Delta\nu/\nu_0)_{para} = (\Delta\nu\ /\ \nu_0)_{hyp} + (\Delta\nu/\nu_0)_{dip} \qquad \text{(A1a)}$$

$$(\Delta\nu/\nu_0)_{dip} = (1/45)\beta^2 S(S+1)(k_B T)^{-1} r_{IS}^{-3}\,(1 - 3\cos^2\theta)(g_{\parallel} - g_{\perp})(3g_{\parallel} + 4g_{\perp}) \qquad \text{(A1b)}$$

$$(\Delta\nu/\nu_0)_{\rm hyp} = -(1/45)\beta S(S+1)(\hbar\gamma_{\rm H}k_{\rm B}T)^{-1}(3g_{\|} + 2g_{\perp})A \tag{A1c}$$

where $(\Delta\nu/\nu_0)_{\rm hyp}$ and $(\Delta\nu/\nu_0)_{\rm dip}$ indicate the shifts caused by the hyperfine and the dipolar interaction, respectively. $(\Delta\nu/\nu_0)_{\rm para}$ for bfc$^+$ and fc$^+$ were determined from the shift difference between bfc$^+$ and bfc or fc$^+$ and fc. In the case of bfc$^+$, the doubled values of the observed shift difference were used for $(\Delta\nu/\nu_0)_{\rm para}$ because the NMR spectra of the cyclopentadienyl protons were averaged over those in the fc and the fc$^+$ sites[52] (see Figure 2). Thus, experimentally obtained $(\Delta\nu/\nu_0)_{\rm para}$ values were compared with the $(\Delta\nu/\nu_0)_{\rm dip}$ values calculated according to eq A1b with the *g* values determined by the ESR and the crystal structural data.[18d,e] The results shown in Tables 1 and 2 indicate that the contribution of the dipolar interaction to the $(\Delta\nu/\nu_0)_{\rm para}$ term for both fc$^+$ and bfc$^+$ is negligible. Thus, the shift is mainly attributed to the hyperfine term, $(\Delta\nu/\nu_0)_{\rm hyp}$. The hyperfine coupling constant can then be obtained from the observed shifts and the *g* values according to eq A1c.

References and Notes

(1) See for example: (a) *Dynamics and Mechanisms of Photoinduced Electron Transfer and Related Phenomena;* Mataga, M., Okada, T., Masuhara, H., Eds.; Elsevier: Amsterdam, 1992. (b) Barbara, P. F.; Jarzeba, W. *Adv. Photochem.* **1990**, *15*, 1.

(2) (a) Kosower, E. M.; Huppert, D. *Annu. Rev. Phys. Chem.* **1986**, *37*, 127. (b) Maroncelli, M.; MacInnis, J.; Fleming, G. R. *Science* **1989**, *243*, 1670. (c) Weaver, M. J.; McManis, G. E. *Acc. Chem. Res.* **1990**, *23*, 294. (d) Barbara, P. F.; Walker, G. C.; Smith, T. P. *Science* **1992**, *256*, 975. (e) Heitele, H. *Angew. Chem., Int. Ed. Engl.* **1993**, *32*, 359.

(3) Bolton, J. R.; Mataga, N.; McLendon, G. *Electron Transfer in Inorganic, Organic, and Biological Systems*; American Chemical Society: Washington, DC, 1991.

(4) Jortner, J.; Bixon, M. *Protein Structure; Molecular and Electronic Reactivity*; Austin, R., Buhks, E., Chance, B., Voult, D., Dutton, P. L., Fauenfelder, H., Gol'danski, V. I., Eds.; Saringer: New York, 1987; p 277.

(5) (a) Robin, M. B.; Day, P. *Adv. Inorg. Chem. Radiochem.* **1967**, *10*, 247. (b) Creutz, C. *Prog. Inorg. Chem.* **1983**, *30*, 1.

(6) (a) Jordan, K. D.; Paddon-row, M. N. *Chem. Rev.* **1992**, *92*, 395. (b) Nelsen, S. F. *Adv. Electron Transfer Chem.* **1993**, *3*, 167.

(7) The largest rate constants of this type of ET reported previously are $\sim 10^{10}$ s^{-1} by the ESR line broadening measurements. (See: Grampp, G.; Jaenicke, W. *Ber. Bunsen-Ges. Phys. Chem.* **1991**, *95*, 9094.)

(8) See for example: Zundel, G.; Fritsch, J. In *Studies in Physical and Theoretical Chemistry 38. The Chemical Physics of Solvation Part B*; Ulstrup, K., Ed.; Elsevier: Amsterdam, 1986; Chapter 2.

(9) (a) Levich, V. G. In *Kinetics Chemistry of Reactions with Charge Transport*; Eyring, H., Henderson, D., Jost, W., Eds.; Academic Press: New York, 1970; Vol. 9B, p 985. (b) Weaver, M. J. *Chem. Rev.* **1992**, *92*, 463. (c) Perez, V.; Luch, J. M.; Bertram, J. *J. Mol. Liq.* **1995**, *63*, 77 and references therein.

(10) (a) Nielsen, R. M.; McManis, M.; Golovin, M. N.; Weaver, M. J. *J. Phys. Chem.* **1988**, *92*, 3441. (b) Gennett, T.; Milner, F.; Weaver, M. J. *J. Phys. Chem.* **1985**, *89*, 2787. (c) McManis, G. E.; Weaver, M. J. *J. Chem. Phys.* **1989**, *90*, 912. (d) Phelps, D. K.; Weaver, M. J. *J. Phys. Chem.* **1992**, *96*, 7187. (e) McManis, G. E.; Gochev, A.; Nielson, R. M.; Weaver, M. J. *J. Phys. Chem.* **1989**, *93*, 7733.

(11) The effect of the diffusion process and the distribution between the donor and acceptor at their close distance is another important subject for intermolecular ET studies. (See for example: (a) Rice, S. A. *Diffusive-Limited Reactions*; *Comprehensive Chemical Kinetics Vol. 25*; Elsevier: Amsterdam, 1985. (b) Tachiya, M. *J. Phys. Chem.* **1993**, *97*, 5911. (c) *J. Phys. Chen.* **1989**, *93*, 7050. (d) Sumi, H. *J. Phys. Chem.* **1991**, *95*, 3334.)

(12) Farrar, T. C.; Becker, E. D. *Pulse and Fourier Transform NMR*; Academic Press: New York, 1971; Chapter 4.

(13) (a) Abragam, A. *Principles of Nuclear Magnetism*; Oxford University Press: Oxford, 1961; Chapter VIII. (b) Boere, R. T.; Kidd, R. G. *Annu. Rep. NMR Spectrosc.* **1982**, *13*, 319.

(14) (a) Steele, W. A. *Adv. Chem. Phys.* **1986**, *34*, 1. (b) Masuda, Y.; Yamatera, H. In *Structure and Dynamics of Solution*; Ohtaki, H., Yamatera, H., Eds., Elsevier: Amsterdam, 1992; Chapter 4.

(15) The NMR spin–spin relaxation time, T_2, or the line broadening has been widely used for determination of chemical reaction rates with a time scale slower than $\sim 10^{-5}$ s.

(16) Hertz, H. G. In *The Chemical Physics of Solvation. Part B*; Dogonadze, R. R., Kalman, E., Kornyshev, A. A., Ulstrap, J., Eds.; Elsevier: Amsterdam, 1986; Chapter 7.

(17) Powell, D. H.; Helm. L.; Merbach, A. E. *J. Chem. Phys.* **1991**, *95*, 9258.

(18) (a) Kaufman, F.; Cowan, D. O. *J. Am. Chem. Soc.* **1970**, *92*, 6198. (b) Cowan, D. O.; Condela, G. A.; Kaufman, F. *J. Am. Chem. Soc.* **1971**, *93*, 3889. (c) Morrison, W. H.; Hendrickson, D. N. *Inorg. Chem.* **1975**, *14*, 2331. (d) Dong, T. Y.; Kambara, T.; Hendrickson, D. N. *J. Am. Chem. Soc.* **1986**, *108*, 4423. (e) Lowey, M. D.; Hammack, W. S.; Drickamer, H. G.; Hendrickson, D. N. *J. Am. Chem. Soc.* **1987**, *109*, 8019.

(19) (a) Dong, T. Y.; Kambara, T.; Hendrickson, D. N. *J. Am. Chem. Soc.* **1986**, *108*, 5857. (b) Nakashima, S.; Masuda, Y.; Motoyama, I.; Sano, H. *Bull. Chem. Soc. Jpn.* **1987**, *60*, 1673. (c) Dong, T. Y.; Hendrickson, D. N.; Pierpont, C. G.; Moore, M. F. *J. Am. Chem. Soc.* **1985**, *107*, 4777.

(20) (a) Cowan, D. O.; Collins, R. L.; Kaufmann, F. *J. Phys. Chem.* **1971**, *75*, 2025. (b) Morrison, W. H.; Hendrickson, D. N. *J. Chem. Phys.* **1974**, *59*, 380. (c) LeVanda, C.; Bechgaard, K.; Cowan. D. O.; Mueller-Westerhoff, U. T.; Eilbracht, P.; Candela, G. A.; Collins, R. L. *J. Am. Chem. Soc.* **1976**, *98*, 3181. (d) Kramer, J. A.; Hendrickson, D. N. *Inorg. Chem.* **1980**, *19*, 3330.

(21) (a) Rausch, M. D. *J. Org. Chem.* **1961**, *26*, 1802. (b) Fish, R. W.; Rosenblum, M. *J. Org. Chem.* **1965**, *30*, 1253. (c) Shechter, H.; Helling, J. F. *J. Org. Chem.* **1961**, *26*, 1034.

(22) bfc$^+$BF$_4^-$ and fc$^+$PF$_6^-$ were prepared according to ref 18e with minor modifications.

(23) Swift, T. J.; La Mar, G. N. In *NMR of Paramagnetic Molecule;* La-Mar, G. N., Horrocks Jr., W. D., Holm, R. H., Eds.; Academic Press: New York, 1973; Chapters 1 and 2.

(24) Banci, L.; Bertini, I.; Luchinat, C. *Nuclear and Electron Relaxation;* VCH Publishers: New York, 1991; Chapter 5.

(25) The inverse of the observed T_1 value, $T_{1\ \rm obs}{}^{-1}$, is an average of those for the cyclopentadienyl protons of the fc$^+$ and the fc unit in bfc$^+$. The paramagnetic contribution to the $T_1{}^{-1}$ for the fc unit is negligibly small compared with that for the fc$^+$ unit because of the much smaller $r_{\rm IS}{}^{-6}$ or A values for the former than the latter. (See eqs 2 and 3.) Thus, the $T_{1\ \rm para}{}^{-1}$ value of the protons in the fc$^+$ unit can be approximated by twice of $T_{\rm 1obs}{}^{-1}$, i.e., $2T_{\rm 1obs}{}^{-1} = T_{\rm 1para}{}^{-1}$.

(26) Prins, R.; Reinders, F. J. *J. Am. Chem. Soc.* **1969**, *91*, 4929.

(27) The correlation time for the $T_{\rm 1hyp}{}^{-1}$ term, $\tau_{\rm c2}'$, is distinct from those for the $T_{\rm 1dip}{}^{-1}$ term in lack of the contribution of the molecular reorientation. (See eq 4.) In the present system, however, the $\tau_{\rm c2}'$ value can be regarded as similar to $\tau_{\rm c2}$ because of $\tau_{\rm r}{}^{-1} \ll T_{\rm 2e}{}^{-1}$ or $k_{\rm et}$ as discussed below. Then, the inside of the brackets of eq 2b is smaller than that of eq 2a. Thus, $T_{\rm 1para}{}^{-1}$ is approximately equal to $T_{\rm 1dip}{}^{-1}$ if $K_{\rm dip}$ is much larger than $K_{\rm hyp}$.

(28) If the electron relaxation time significantly contributes to $\tau_{\rm c1}$ or $\tau_{\rm c2}$, i.e., $T_{\rm 1e}$, $T_{\rm 2e} \ll 10^{-11}$–10^{-12} s, solvent collision or vibrational relaxations with time scale of 10^{-12} s order or less are responsible for the electron relaxation. (Banci, L.; Bertini, I.; Luchinat, C. *Nuclear and Electron Relaxation,* VCH Publishers: New York, 1991; Chapter 4). In this situation, $T_{\rm 2e}$ is not much smaller than $T_{\rm 1e}$ under the condition $\omega_{\rm s} = 1 \times 10^{12}$ s^{-1} in the present study.

(29) If $T_1 > T_2$, i.e., $\omega_{\rm S}{}^2\tau_{\rm c}{}^2 \geq 1$, the difference between the T_1 and T_2 values gives the correlation time without information on the parameters such as the *g* values, etc. The observed T_2 values were 6–8 times shorter than the T_1 values at room temperature in most of the solvents. However, this excess decrease in T_2 can be attributed to the intermolecular ET of bfc$^+$ with bfc or bfc^{2+}, which is produced by the disproportionation of bfc$^+$, i.e., 2bfc$^+ \rightleftharpoons$ bfc^{2+} + bfc, and is examined as follows. The intermolecular ET rate was estimated with the disproportionation constants of the above equilibrium, which was calculated from the redox potentials (ref 18b), and the intermolecular ET rate constants, which are assumed to be equal in the fc–fc$^+$ system (ref 10). The estimated fractions of bfc or bfc^{2+} were less than 5%, and this gave the lifetime of bfc$^+$, e.g., $\sim 10^{-3}$ s^{-1} in 1 mM bfc$^+$ solution of acetone at room temperature. The effect of these intermolecular ET's was actually observed in the slight increase of $T_2{}^{-1}$ compared to $T_1{}^{-1}$ for example in acetone in the temperature range 270–300 K but is negligible to the obtained T_1.

(30) For bfc$^+$ or fc$^+$, an isotropic overall rotation and a rotation of the cyclopentadienyl ring around the pseudo-C_5 axis are assumed. A negligible effect of anisotropy for the overall rotation of bfc$^+$ (or bfc) is supported by similar $\tau_{\rm r(eff)}$ values (in eq 5) for the two kinds of the fulvalene protons of bfc. (See Table 1.) The correlation times of the rotation of the vectors connecting the electron spin, i.e., the Fe(III) ion and the cyclopentadienyl protons in the fc$^+$ unit of bfc$^+$, which are responsible for $T_{\rm 1dip}$ ($\tau_{\rm r}$ in eq 4), were calculated according to a representation in the literature (ref 14a) with the $\tau_{\rm r(eff)}$ values of the cyclopentadienyl and the fulvalene protons.

(31) (a) Masuda, Y.; Yamatera, H. *J. Phys. Chem.* **1983**, *87*, 5339. (b) Masuda, Y.; Yamatera, H. *J. Phys. Chem.* **1984**, *88*, 3425.

(32) Maki, A. H.; Berry, T. E. *J. Am. Chem. Soc.* **1965**, *87*, 4437.

(33) Burton, W.; Morgan, L. O. In *Transition Metal Chemistry;* Carlim, R., Ed.; Marcel Dekker: New York, 1968; Vol. 4, pp 33.

(34) The temperature and solvent dependences of the *g* values and the hyperfine coupling constants, *A*, were disregarded. The $\tau_{\rm r}$ values in the solvents other than acetone are listed in Table 3.

(35) McManis, G. E.; Nielson, R. M.; Weaver, M. J. *Inorg. Chem.* **1988**, *27*, 1827.

(36) Gachter, B. F.; Koningstein, J. A. *J. Chem. Phys.* **1975**, *62*, 4628.

(37) The slight temperature dependences of λ_{os} in various solvents were estimated by those of the static dielectric constants, ϵ_s, with the relation, $\lambda_{os} \propto 1/\epsilon_{op} - 1/\epsilon_s$, regarding solvents as a dielectric continuum. (ϵ_{op} indicates the optical dielectric constant.) The temperature dependences of λ_{is}, H_{12}, and ϵ_{op} were disregarded.

(38) (a) Rips, I.; Jortner, J. *J. Chem. Phys*. **1987**, *87*, 2090. (b) Van der Zwan, G.; Hynes, J. T. *J. Phys. Chem*. **1985**, *89*, 4181. (c) Hynes, J. T. *J. Phys. Chem*. **1986**, *90*, 3701.

(39) (a) Sumi, H.; Marcus, R. A. *J. Chem. Phys*. **1986**, *84*, 4247. (b) *J. Chem. Phys.* **1986**, *84*, 4896.

(40) Sumi, H. *J. Mol. Liq.* **1995**, *65*, 65. (b) *J. Phys. Chem*. **1996**, *100*, 4831. (c) Sumi, H.; Asano, T. *J. Chem. Phys*. **1995**, *102*, 9565.

(41) Phelps, D. K.; Weaver, M. J. *J. Phys. Chem*. **1992**, *96*, 7187.

(42) Zhu, J.; Rasaiah, J. C. *J. Phys. Chem.* **1991**, *95*, 3325.

(43) Scrupulous calculations of the ν_n values according to ref 38b considering the contribution of nonadiababicity gave similar results.

(44) (a) Akesson, E.; Walker, G. C.; Barbara, P. F. *J. Chem. Phys*. **1991**, *95*, 4188. (b) Akesson, E.; Jhonson, A. E.; Levinger, N. E.; Walker, G. C.; DuBruil, T. P.; Barbara, P. F. *J. Chem. Phys.* **1992**, *96*, 7859.

(45) (a) Tominaga, K.; Kliner, D. A. V.; Johnson, A. E.; Levinger, N. E.; Barbara, P. F. *J. Chem. Phys*. **1993**, *98*, 1228. (b) Kliner, D. A. V.; Tominaga, K.; Walker, G. C.; Barbara, P. F. *J. Am. Chem. Soc*. **1992**, *114*, 8323.

(46) Jortner, J.; Bixon, M. *J. Chem. Phys*. **1988**, *88*, 167.

(47) (a) Weaver, M. J.; McManis, G. E.; Jarzeba, W.; Barbara, P. F. *J. Phys. Chem*. **1990**, *94*, 1715. (b) *J. Phys. Chem*. **1986**, *90*, 6563.

(48) (a) Barthel, J.; Bachhuber, K.; Buchner, R.; Hetzenauer, H. *Chem. Phys. Lett*. **1990**, *165*, 369. (b) Maroncelli, M. *J. Mol. Liq*. **1993**, *57*, 1. (c) Bagchi, B.; Chandra, A. *Adv. Chem. Phys*. **1991**, *80*, 1.

(49) (a) Rosenthal, S. J.; Xie, X.; Du, M.; Fleming, G. R. *J. Chem. Phys.* **1991**, *95*, 4715. (b) Kahlow, M. A.; Kang, T. J.; Barbara, P. F. *J. Chem. Phys.* **1987**, *86*, 3183. (c) Jarzzeba, W.; Walker, G. C.; Johonson, A. E.; Kahlow, M. A.; Barbara, P. F. *Chem. Phys.* **1991**, *152*, 111.

(50) McMorrow, D.; Lotsaw, W. T. *J. Phys. Chem.* **1991**, *95*, 10395.

(51) The quantization axis for the dipolar interaction was assumed to be along the main axis of the **g** tensor because the rotational correlation time is significantly longer than the electron spin relaxation time. (See section 3.2 and Table 1.) The isotropic hyperfine interactions were also assumed.

(52) The NMR shift ($\Delta\nu/\nu_o$) can be represented by a sum of the diamagnetic and the paramagnetic contribution, i.e., $\Delta\nu/\nu_o = (\Delta\nu/\nu_o)_{dia} + (\Delta\nu/\nu_o)_{para}$. The observed resonance of the cyclopentadienyl protons is an average of those for the fc$^+$ and the fc unit in bfc$^+$. If $(\Delta\nu/\nu_o)_{dia}$ of the protons in the fc$^+$ unit of bfc$^+$ is similar to that in the fc unit and $(\Delta\nu/\nu_o)_{para}$ in the fc unit is negligibly small compared with that in the fc$^+$ unit, the $(\Delta\nu/\nu_o)_{para}$ in the fc$^+$ unit is approximated by twice of the shift difference between bfc$^+$ and bfc. (See Table 1.)